Triply excited ^4S resonances of He^-

N. Brandefelt and E. Lindroth
Atomic Physics, Department of Physics, SCFAB, Stockholm University, S-106 91 Stockholm, Sweden
(Received 6 June 2001; published 6 February 2002)

Resonances of $^4S^e$ symmetry in He^- are searched for in the region above the $He^+(n=1)$ threshold and below the $He^+(n=2)$ threshold. The energies and widths of the resonances are calculated with an *ab initio* three-electron description of the ion. The complex rotation method is combined with the use of *B* splines in a spherical cavity to describe the ion and the decay channels. Seven resonances are found and five are presented with energy position and width.

DOI: 10.1103/PhysRevA.65.032503 PACS number(s): 31.15.Ar, 31.25.Jf, 32.80.Dz

I. INTRODUCTION

As a test case for how well computational methods can handle three electrons the He^- system should be ideal. Compared to H^-, used as a test case for two-electron effects, He^- is even more fragile since it lacks the degenerate states in the parent atom, and thus the dipole potential felt by the outermost electron is even weaker than in H^-. As pair correlation is enhanced in doubly excited states, triply excited states should reveal three-electron effects. The best test case for three-electron effects would then be triply excited states in He^-.

Several triply excited states of He^- have already been measured and calculated. The position and width of the triply excited state $(2s^22p)^2P$ of He^- was measured already in the seventies [1,2] and it has recently been reinvestigated theoretically [3,4]. Another measurement also carried out in the seventies found triply excited states [5], but had to wait until quite recently for theoretical confirmation and interpretation [6]. Features were found just below and above the $He(3s^2\,^1S)$ threshold. Also the $(2p^3)\,^4S$ state has been detected [7,8] following predictions by calculations [9–13].

He^- has no bound state, but the lowest energy $^4P^o$ state is metastable since it is bound below the lowest triplet state in helium $(1s2s)\,^3S$ and can only autodetach by a spin flip. This long-lived state can be used for photodetachment studies. Several laser technique investigations of autodetaching states in He^-, above the single ionization threshold but below the double-ionization threshold, have been published [14–17]. Several theoretical investigations of He^- have also been carried out [18–26]. Even if the above experiments have not been performed with high enough photon energies to reach the triply excited states, it should in principle be possible to do such an experiment, either by using a high-order harmonic of an intense pulsed tunable laser [27], or by using synchrotron radiation.

In an earlier publication, we searched He^- for doubly excited states of $^4S^e$ symmetry below the $He^+(n=1)$ threshold [22]. In this paper, we will use the same method to study the region above the $He^+(n=1)$ threshold and below the $He^+(n=2)$ to find triply excited states, again of $^4S^e$ symmetry. The $He^+(n=1)$ and $He^+(n=2)$ thresholds are 4.8 eV and 46 eV above the metastable $(1s2s2p)^4P$ state of He^-, respectively. Previous theoretical studies of triply excited resonances with $^4S^e$ symmetry has been made by Xi and Froese Fisher [25], who list one such resonance, and very recently by Zhou *et al* [26]. In our method complex rotation combined with *B*-spline basis functions in a spherical cavity are used to construct the three-electron matrix, which is then diagonalized. All three electrons are treated equivalently. Seven resonances are found and five are presented with energy position and width.

The method is described in Sec. II and the results are discussed in Sec. III and compared with other theoretical calculations in Sec. IV.

II. METHOD

The present calculation combines complex rotation with *B* splines in a spherical cavity. The nonrelativistic three-electron Hamiltonian in the limit of infinite nuclear mass reads (in a.u. $e=m_e=\hbar=4\pi\epsilon_0=1$)

$$H=h_1+h_2+h_3+\frac{1}{r_{12}}+\frac{1}{r_{23}}+\frac{1}{r_{31}}, \tag{1}$$

where

$$h_i=\frac{p_i^2}{2}-\frac{Z}{r_i}, i=1,2,3. \tag{2}$$

This Hamiltonian is diagonalized using eigenfunctions to $h_1+h_2+h_3$ coupled to a specific total symmetry, as a basis set,

$$\{\langle[(n_a l_a n_b l_b)^{S'}L' n_c l_c]^S L|\}H\{|[(n_d l_d n_e l_e)^{S''}L'' n_f l_f]^S L\rangle\}. \tag{3}$$

All angular integrals are performed analytically using Racah algebra [28]. The functions $P_{n,l}(r)=rR_{n,l}(r)$ are expanded in *B* splines [29] [$R_{n,l}(r)$ is the radial part of the one-electron wave function]. The Rayleigh-Ritz-Galerkin scheme is used to convert the differential equation for $P_{n,l}(r)$ to a symmetric generalized eigenvalue equation.

To construct *B* splines a set of points $\{t_i\}$, called the knot set, is defined on a given interval, in this case $[0,R]$, where *R* is the size of the cavity. The only necessary restriction on the knot set is that $t_i \leqslant t_{i+1}$. *B* splines of order *k* can now be defined recursively as

$$B_{i,1}(x)=\begin{cases}1 & \text{if } t_i \leqslant x < t_{i+1},\\ 0 & \text{otherwise,}\end{cases} \tag{4}$$

$$B_{i,k}(x)=\frac{x-t_i}{t_{i+k-1}-t_i}B_{i,k-1}(x)+\frac{t_{i+k}-x}{t_{i+k}-t_{i+1}}B_{i+1,k-1}(x). \tag{5}$$

In the present calculation B splines of order $k=5$ are used, and 5 knots are put at $r=0$ and $r=R$. All other knot points appear only once. The first and last spline are removed from the basis set. These are the only splines that are nonzero at $r=0$ and at $r=R$ and by removing them the boundary conditions $P_i(0)=P_i(R)=0$ are enforced. This is the same scheme used by Johnson *et al.* [30,31], who pioneered the use of B splines in atomic calculations.

The reason that we first diagonalize the radial part of the one-electron Hamiltonian and then use the eigenstates to diagonalize the three-electron Hamiltonian instead of using the B splines directly is that it turns out that the one-electron eigenstates with highest principle quantum numbers can be removed from the basis set when constructing the three-electron basis set without affecting the resonant states of interest and thus saving valuable memory space.

To be able to describe autodetaching states, the continuum of outgoing electrons is needed. These functions are not square integrable and complex rotation is used to represent these states in a limited cavity. With this widely used method the radial coordinates in the Hamiltonian are rotated, $r\rightarrow re^{i\vartheta}$ [32]. Recent calculations using complex rotation in the treatment of He^- are found in Refs. [3,4,21,22]. A recent example of complex rotation in combination with B splines can be found in Refs. [33,34]. The complex rotation method allows energy and half width of a resonance to be calculated as the real and imaginary part of a complex eigenvalue. The calculated width is the total width for autodetachment only, since the radiation field is not included in the Hamiltonian. Theoretically, the result of a complex rotation calculation should be independent of the angle ϑ used. In a numerical calculation this is never completely true. A small angular dependence is introduced because of limitations in the numerical description. The most correct eigenvalue is obtained when the calculated eigenvalue is stationary with respect to ϑ as discussed in Refs. [35,36].

The crucial point in these calculations is the approximation made by describing the radial coordinates with a certain set of B splines. The three-particle matrix to diagonalize, cf., Eq. (3), grows rapidly with the number of B splines used and it is essential to minimize the number of B splines needed to describe the system at a given level of accuracy. For this the knot set must be carefully chosen. Three different regions are used here. In region one, close to the nucleus, the knot sequence is linear. In the second region the knot sequence is exponential, and in the third region there are no knot points except on the boundary. The localized part of the resonances is negligible in the last region, but the region is needed to describe the decay channels. We have further investigated different choices of the order k of the B splines and found that $k=5$ is the best choice for our optimized knot sequence.

TABLE I. Energy and width of the ^4S resonances in He^- obtained in the present calculation. Energy position is relative to complete breakup. The number of digits reflects the estimated errors as discussed in Sec. III.

Resonance	E (a.u.)	Γ (a.u.)
1	-0.602648	1.3×10^{-5}
2	-0.58694	7.66×10^{-3}
3	-0.56083	2.96×10^{-4}
4	-0.55011	8.0×10^{-4}
5	-0.54347	1.34×10^{-3}

III. RESULTS

Seven resonances with $^4S^e$ symmetry are found above the $He^+(n=1)$ threshold and below the $He^+(n=2)$ threshold. This search does not in any way show that these are the only resonances. On the contrary, we find some evidence for more resonances. Two of the seven resonances we have not been able to calculate to any accuracy due to computer limitations. They are situated approximately at -0.534 a.u., and -0.531 a.u. and will not be addressed further in this paper. The energy and widths of the other five resonances are presented in Table I. Different parameters used in the calculation of the five resonances are give in Table II. To find the optimal angle of complex rotation the same parameters were used for all five resonances. The size of the cavity was 332 a.u., the number of B splines was 19 and the number of one-electron eigenfunctions for each n was $P_{n,l}=16$. The angular configurations sss, spp, sdd, and ppd were included. Similar parameters were then used to test which additional angular configurations needed to be included for each resonance. To the four configurations, sss, spp, sdd, and ppd, other configurations were added one at a time. The result of this can be seen in Table III.

To be able to include all three electrons on the same footing the number of B splines have to be kept as small as possible. In order to estimate the errors introduced due to this limitation and also from the limited cavity size and the cut in the number of one-electron basis functions used, these parameters have been increased one at a time. To test these limitations, the same parameters that were used above to find the optimal angle of complex rotation was used as a starting point for the same four angular configurations. These tests will be carefully described for the first resonance and the main results mentioned for the four other resonances. First, we used all 19 one-electron eigenfunctions and compared the result with the result when we used only 16. The difference is then 3×10^{-8} a.u. for the position and 6×10^{-8} a.u. for the width. We then also included 17 and 18 one-electron eigenfunctions to check the convergence of our results. We then increased the size of the cavity to the next exponential point in the grid, that is to approximately 462 a.u. The difference obtained between the two cavity sizes was 6×10^{-8} a.u. for the position and 5×10^{-7} a.u. for the width. As the aim here was to get an idea of the size of the errors, we did not keep increasing the cavity until it had no effect but only tried to add one point more at approximately 643 a.u. The difference

TABLE II. Parameters used in the calculations of the resonances energies and widths. ϑ is the complex rotation angle. R is the cavity size. Number of $P_{n,l}$ is the number of one-electron wave functions actually used to create the three-electron basis, e.g., for resonance 1, no. of B splines $=19$ and no. of $P_{n,l}=16$ mean that the three wave functions with highest principal quantum numbers are discarded (not the three last B splines).

Resonance	ϑ	R (a.u.)	No. of B splines	No. of $P_{n,l}$	Configurations
1	12.5°	332	19	16	sss,spp,sdd ppd,pdf
2	25°	332	19	15	sss,spp,sdd ppd,ddd,ffs pdf
3	17°	332	19	15	sss,spp,sdd ppd,ffs,pdf pfg
4	18°	332	20	16	sss,spp,sdd ppd,ffs,pdf
5	17°	332	21	17	sss,spp,sdd ppd,ddd,ffs pdf

[a]For angular configuration ppd, ddd, ffs, and pdf the number of one-electron wave functions was only 16 for this resonance.

from the calculation with cavity size 462 a.u. was then 2×10^{-8} a.u. for the position and 1×10^{-8} a.u. for the width. Next, we tested the B-splines basis. This was done separately for each region. First, we included exponential knot points in the region where we have no points in the final calculation. This makes a difference of 5×10^{-8} a.u. for the position and 8×10^{-8} a.u. for the width. Then we increased the number of knot points in the linear region closest to the nucleus. We increased it first with two points and then with three points. The main difference comes already when we add two points. This is of course no proof of convergence but gives a hint about the error we make. The difference between

TABLE III. Complex eigenvalue, given in a.u., of each resonance when different angular configurations are added, one at a time, to the four most important configurations. This is done to see which configurations are needed in the final calculation. The real part is given first and corresponds to the energy position. The imaginary part is given just below and corresponds to the half width. Atomic units are used. All calculations in this table are done with cavity size $R=332$ a.u. and no. of B splines$=19$. The number of one-electron wave functions included for each n is 16 for resonance 1 and 15 for the rest. The complex rotation angle is 10° for resonance 1, 25° for resonance 2, and 17° for resonances 3, 4, and 5.

Configurations	Resonance 1	Resonance 2	Resonance 3	Resonance 4	Resonance 5
sss,spp	-0.60264248	-0.58668066	-0.56033381	-0.54998913	-0.54319794
sdd,ppd	-6.367×10^{-6}	-3.832×10^{-3}	-1.374×10^{-4}	-4.879×10^{-4}	-6.057×10^{-4}
$+ddd$	-0.60264259	-0.58672632	-0.56033478	-0.54999204	-0.54322073
	-6.367×10^{-6}	-3.784×10^{-3}	-1.384×10^{-4}	-4.855×10^{-4}	-6.262×10^{-4}
$+ffs$	-0.60264716	-0.58671285	-0.56037874	-0.54999546	-0.54319525
$(+ddd)$ [a]	-6.384×10^{-6}	-3.848×10^{-3}	-1.370×10^{-4}	-4.477×10^{-4}	-7.578×10^{-4}
$+pdf$	-0.60264841	-0.58685833	-0.56077704	-0.55010236	-0.54327035
$(+ddd)$ [a]	-6.525×10^{-6}	-3.874×10^{-3}	-1.487×10^{-4}	-4.286×10^{-4}	-5.633×10^{-4}
$+ffd$	-0.60264249	-0.58668335	-0.56033383	-0.54998944	-0.54319865
	-6.367×10^{-6}	-3.831×10^{-3}	-1.374×10^{-4}	-4.877×10^{-4}	-6.072×10^{-4}
$+pfg$	-0.60264302	-0.58669561	-0.56036986	-0.54999864	-0.54320469
	-6.380×10^{-6}	-3.837×10^{-3}	-1.287×10^{-4}	-4.769×10^{-4}	-6.053×10^{-4}
$+ggs$	-0.60264300	-0.58668636	-0.56034273	-0.54998910	-0.54319911
	-6.370×10^{-6}	-3.836×10^{-3}	-1.373×10^{-4}	-4.852×10^{-4}	-6.166×10^{-4}
$+ddg$	-0.60264249	-0.58668191	-0.56033381	-0.54998984	-0.54319582
	-6.367×10^{-6}	-3.831×10^{-3}	-1.373×10^{-4}	-4.814×10^{-4}	-6.092×10^{-4}

[a]For resonance 1 the ddd configuration was also included in this calculation.

the best and worst grid in the result was 5×10^{-8} a.u. for the position and 2×10^{-7} a.u. for the width. Finally, we added exponential points in the middle part of the knot sequence. Here we added first one then two and finally three knot points. The width seemed to oscillate as we added points. We started with 1.27×10^{-5} a.u. when we added one point we got 1.23×10^{-5} a.u., two points 1.27×10^{-5} a.u., and three points 1.25×10^{-5} a.u. As the oscillation seems to decrease we will take the difference between the maximum and minimum value as an estimate of the error, 4×10^{-7} a.u. The position does not oscillate but the difference is quite large. The maximum difference between the grids used was 1×10^{-6} a.u. Last we looked at the error caused by not including some angular configurations as can be estimated from Table III. For resonance 1 the largest error comes from not including ffs and it is 5×10^{-6} a.u. in position and 4×10^{-8} a.u. in width. In conclusion, we have a rough error estimate of 5×10^{-6} a.u. in position and 1×10^{-6} a.u. in the width for resonance 1.

In the calculation of resonance 2 the largest errors are due to the small B-spline set. When the number of exponential knot points are increased the position changes with 3×10^{-5} a.u. The second largest error in position comes from not including the pfg configuration and it is 2×10^{-5} a.u. The largest error in the width comes from the outer region where no knot points are situated. When points are added here the change in width is 1×10^{-4} a.u. In conclusion, we have an error estimate of 4×10^{-5} a.u. for the position and 1×10^{-4} a.u. for the width.

For resonance 3 the largest error in position comes from not including the sgg configuration and it is 1×10^{-5} a.u. The largest errors in the width comes from the limited cavity size and from not including the ddd configuration. Each gives an error of approximately 2×10^{-6} a.u. The final error estimate is 1×10^{-5} a.u. for the position and 3×10^{-6} a.u. for the width.

Resonance 4 is calculated with only six different angular configurations and this is the main limitation on the accuracy of the result. Not including pfg gives the largest error and it is estimated to be 1×10^{-5} a.u. for the position and 2×10^{-5} a.u. for the width. For the width there is one more large contribution from not including the ddg configuration and it is 1×10^{-5} a.u. The total error is estimated to 1×10^{-5} a.u. for the position and 2×10^{-5} a.u. for the width.

For resonance 5 a compromise was needed. We excluded some important angular configurations, namely, ggs and pfg and we used 17 one-electron eigenfunctions for sss, spp, and sdd and 16 for ppd, ddd, pdf, and ffs. The estimated error due to the inclusion of only 16 one-electron eigenfunctions is 1×10^{-5} a.u. for the position and 2×10^{-5} a.u. for the width. This will be a slightly overestimated error as we do use 17 eigenfunctions for some angular configurations. The second largest error in the position comes from not including pfg and is 7×10^{-6} a.u. The second largest error in the width comes from not including ggs and is 2×10^{-5} a.u. So the final error estimate for the resonance is 1×10^{-5} a.u. for the position and 3×10^{-5} a.u. for the width.

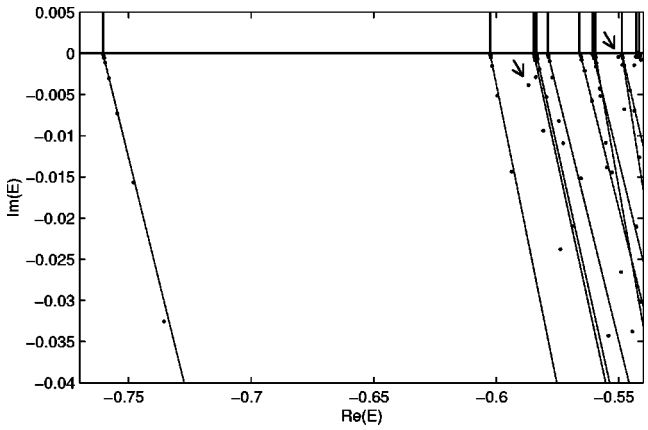

FIG. 1. Complex eigenvalues (in a.u.) from the calculation of resonance 2 are plotted in the region of interest in this article. A help line is drawn for each threshold. This line is drawn through the first two eigenvalues in each continuum. The vertical lines above the x axis are previously published values for the doubly excited states of helium that make up the thresholds [37,38]. They are classified from left to right as $2l2l'\ ^3P^o$, $2l3l'\ ^3S^e$, $2l3l'\ ^3P^o$, $2l3l'\ ^3D^e$, $2l3l'\ ^3P^o$, $2l3l'\ ^3F^o$, $2l3l'\ ^3D^e$, $2l3l'\ ^3S^e$, $2l4l'\ ^3S^e$, $2l3l'\ ^3P^o$, $2l4l'\ ^3P^o$, and $2l4l'\ ^3D^e$. The arrows point at resonance numbers 2 and 4.

In a complex rotation calculation, we do not only get the resonances but also the thresholds. In Fig. 1, the eigenvalues in the region of interest are plotted (these eigenvalues are from the calculation of resonance 2). Each eigenvalue is plotted as a small point in the complex plane. The first threshold is situated at -0.76 a.u. This is the $2s2p^3P$ doubly excited state in helium. The eigenvalues that are situated on the diagonal line originating at this threshold represent eigenstates with helium in $2s2p^3P$ and one free electron. The distance on the real axis between the threshold value and a particular continuum eigenstate represents the kinetic energy of the free electron. When the Hamiltonian is complex rotated these continuum states aquire an imaginary part and the continuum is rotated twice the angle used to complex rotate. In this case the complex rotation angle is $\vartheta=25°$ and the continuum is rotated 50° from the real axis. The lines in this picture are drawn so that they pass through the two continuum states with the lowest energy at each threshold. Continuum states with higher energy deviates more and more from this line. This is due to the fact that they oscillate more and more and the representation becomes less and less perfect. For some thresholds this deviation starts already for the second continuum state and, therefore, these lines show the wrong angle. The straight lines on the positive side of the x axis are earlier published results for the doubly excited states of helium [37,38]. They match up quite well on this scale. In Fig. 1 resonance 2 and 4 can be seen. The other resonances have too small widths and are too close to threshold to be seen.

IV. COMPARISON

In Table IV, the first resonance is compared to another theoretical calculation [25] and the other resonances are also

TABLE IV. Energy positions and widths for five triply excited states of $^4S^e$ symmetry relative to the metastable state $1s2s2p^4P$. For resonance 1, a comparison is also made with an earlier calculation.

	E-$E(1s2s2p)^4P$(eV)	Γ (meV)
Resonance 1		
Present	42.8638	0.35
Xi and Froese Fischer[a]		
Length form	42.86600	0.103
Velocity form	42.86600	0.102
Resonance 2		
Present	43.291	208
Resonance 3		
Present	44.0015	8.06
Resonance 4		
Present	44.2933	22
Resonance 5		
Present	44.4739	36.5

[a]Reference [25].

given for future reference. The nonrelativistic value $-2.178\,077\,6$ a.u. for the energy level $(1s2s2p)^4P$ from Bunge and Bunge [39] (confirmed by Bylicki and Pestka [40]) is used. To convert from a.u. to eV the value 1 a.u. $=27.211\,396(M)/(M+m_e)=27.207\,666$ eV is used. There is a small difference in position and a huge difference in width between our value for the first resonance and the value given by Ref. [25]. After submission of the present work an additional study of He^- [26] was published that found width in good agreement with Ref. [25].

First, we discuss the difference in position that is 2.2 meV. The difference is much larger than can be explained by the estimated uncertainty in the preceding section, which amounts to approximately 0.1 meV. Reference [25] gives also the distance 1.3 meV to the nearest threshold $(2s3s^S)$. This distance in our calculation is 1.8 meV. The difference in binding energy relative to the closest threshold is thus only 0.5 meV that is of the same order as the estimated error in the present calculation. The present value for the threshold is compared to the target state energy of Ref. [25] and to the values obtained in two other calculations in Table V. It is clear that our threshold value is in better agreement and this could support that our absolute energy value is to the same degree better. It is, however, no proof of this, as it is at least in our method sometimes possible to find the position of a resonance with higher absolute accuracy than the accuracy of the nearest threshold. The position found by Ref. [26] deviates with more than 50 meV from what is found here as well as from what is found in Ref. [25]. This difference seems to be dominated by a difference in the threshold position. We must here also mention how we, from our calculation, obtain the threshold. In the complex rotated eigenspectrum there is no eigenstate that corresponds to the threshold. Instead we have several states that correspond to the threshold state and one free electron with some kinetic energy, so-called continuum states. The threshold value is obtained by drawing a line through the two lowest-lying continuum states and determining at which x value it reaches the negative y value that corresponds to the half width of the doubly excited state that makes up the threshold. This point would correspond to helium in the doubly excited state and one free electron with zero kinetic energy [41]. The half width used for the doubly excited state that make up the threshold was -3.32×10^{-6} a.u. from Ref. [37] but the result is not very sensitive to this. If we consider the width to be zero we obtain $-0.602\,586\,6$ a.u. instead of $-0.602\,580\,3$ a.u. for the threshold.

TABLE V. $He(2l3l'^3S^e)$ threshold just above resonance 1 from the calculation of resonance 1 compared with the value given in the calculation of the same resonance in Ref. [25]. Also included are the values obtained in two other calculations of doubly excited states of He. Energy is relative to complete breakup.

	E (a.u.)
Present	-0.6025803
Xi and Froese Fischer[a]	-0.6024865
Oza[b]	-0.602576765
Lindroth[c]	-0.60258

[a]Reference [25].
[b]Reference [38].
[c]Reference [37].

We now like to discuss the huge difference in width. The closest threshold to which this state can decay is the $He(2s2p^3P^o)$ threshold. Other possible decay channels are the double detachment channel leaving the positive ion in $He^+(n=1)$, and all channels leading to singly excited states of helium below this threshold with correct symmetry. The $He(2s2p^3P^o)$ threshold is situated at -0.76 a.u, nine times closer than the double detachment threshold at -2 a.u. A reasonable guess would be that the $He(2s2p^3P^o)$ state is by far the most important decay channel. To test this hypothesis we would like to exclude all other decay channels. What we do is to completely exclude $1s$ from our calculation. Unfortunately, this also affects the $He(2s2p^3P^o)$ threshold. In Fig. 2, we have plotted some of the eigenstates belonging to the $2s2p^3P^o$ threshold from both the normal calculation of resonance 1 and from a calculation that excludes the $1s$ one-electron eigenfunctions. As can be seen the effect is quite small at least compared to the distance to the resonance at $-0.602\,648$ a.u. It is also interesting to note that in the complete calculation the continuum does not go all the way to the x axis indicating that the threshold has an imaginary part, i.e., that it is autoionizing. When $1s$ is excluded this threshold state becomes stable as all the decay channels have disappeared, and the continuum states go all the way to the x axis (or at least one order of magnitude closer). When $1s$ states are excluded resonance 1 is found at $-0.602\,676-i2.3\times10^{-6}$ a.u.. The imaginary part is the half width in atomic units and corresponds to a width of 0.125 meV, i.e., in much better agreement with Ref. [25]. So it turns out that the decay channels including $1s$ states are very important. Some of these but not all are included in the calculation of Ref. [25]. The double detachment threshold are, for example, not

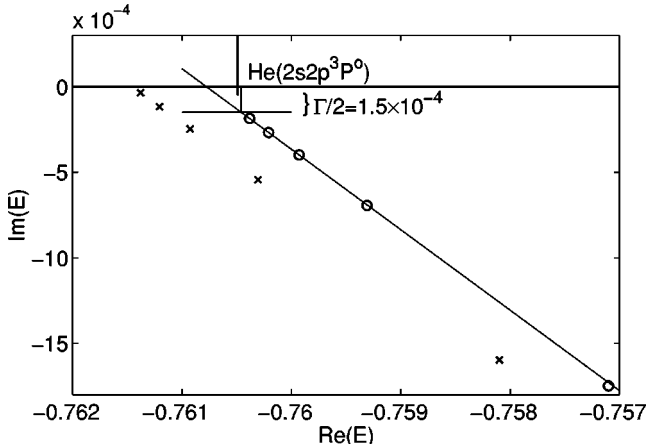

FIG. 2. Complex eigenvalues (in a.u.) in the He($2s2p\ ^3P^o$) threshold region from the complete calculation (represented with o) and from one that excludes all basis states that include any 1s one-electron states (represented with x). The vertical line is the position of the He($2s2p\ ^3P^o$) threshold as published in Ref. [37]. The doubly excited threshold is itself autoionizing and as a consequence the continuum states do not continue all the way up to the real axis. The distance to the real axis agrees well with the half width of He($2s2p\ ^3P^o$) from Ref. [37].

included in their calculation. Since the agreement with Ref. [25] is drastically improved when the 1s states are excluded from the basis set it is tempting to suggest that Ref. [25] misses some important decay channels. Reference [26] finds a width of 0.12 meV, i.e., agreeing rather well with Ref. [25]. However, since similar approximations are made in Ref. [26] regarding, e.g., the neglect of the double detachment channel this does not really add to the understanding of this difference. We unfortunately can not investigate this further as we do not have the possibility to turn on and off different decay channels at will.

We note finally that although Ref. [25] does not list resonance parameters for any other $^4S^e$ states there is a clear indication for resonance 2 in the calculated photodetachment spectrum. Also in Ref. [26] this broad resonance is visible and the position there is given as 43.35 eV in fair agreement with our determination 43.291 eV.

V. CONCLUSION

We have used a true three-electron method to calculate true three-electron states, triply excited states of $^4S^e$ symmetry in He^-. Of five calculated resonances only one has been accurately calculated before. The large deviation in width between the previous published result for resonance 1 and the present is suggested to depend on the fact that the other calculation misses one or more important decay channels. This large deviation also suggest that these states are in fact excellent as test cases for how well we can handle three particle effects and we hope that in the near future this energy regime can be tested experimentally.

ACKNOWLEDGMENT

Financial support for this research was received from the Swedish Research Council (VR).

[1] J. Quéméner, C. Paquet, and P. Marmet, Phys. Rev. A **4**, 494 (1971).
[2] P. Marchand, Can. J. Phys. **51**, 814 (1973).
[3] M. Bylicki and C. A. Nicolaides, Phys. Rev. A **51**, 204 (1995).
[4] Y. Zhang and K. T. Chung, Phys. Rev. A **58**, 3336 (1998).
[5] D. Roy, Phys. Rev. Lett. **38**, 1062 (1977).
[6] C. A. Nicolaides and N. A. Piangos, J. Phys. B **34**, 99 (2001).
[7] E. J. Knystautas, Phys. Rev. Lett. **69**, 2635 (1992).
[8] E. Träbert, P. H. Heckmann, J. Doerfert, and J. Granzow, J. Phys. B **25**, L353 (1992).
[9] D. R. Beck and C. A. Nicolaides, Chem. Phys. Lett. **59**, 525 (1978).
[10] K. T. Chung, Phys. Rev. A **20**, 724 (1979).
[11] C. A. Nicolaides and Y. Komninos, Chem. Phys. Lett. **80**, 463 (1981).
[12] B. F. Davis and K. T. Chung, Phys. Rev. A **42**, 5121 (1990).
[13] C. A. Nicolaides, J. Phys. B **25**, L91 (1992).
[14] C. W. Walter, J. A. Seifert, and J. R. Peterson, Phys. Rev. A **50**, 2257 (1994).
[15] A. E. Klinkmüller *et al.*, Phys. Rev. A **56**, 2788 (1997).
[16] A. E. Klinkmüller *et al.*, J. Phys. B **31**, 2549 (1998).
[17] I. Y. Kiyan, U. Berzinsh, D. Hanstorp, and D. J. Pegg, Phys. Rev. Lett. **81**, 2874 (1998).
[18] S. I. Themelis and C. A. Nicolaides, J. Phys. B **28**, L379 (1995).
[19] J. Xi and C. F. Fischer, Phys. Rev. A **53**, 3169 (1996).
[20] D. S. Kim, H. L. Zhou, and S. T. Manson, Phys. Rev. A **55**, 414 (1997).
[21] M. Bylicki, J. Phys. B **30**, 189 (1997).
[22] N. Brandefelt and E. Lindroth, Phys. Rev. A **59**, 2691 (1999).
[23] C. N. Liu and A. F. Starace, Phys. Rev. A **60**, 4647 (1999).
[24] C. A. Ramsbottom and K. L. Bell, J. Phys. B **32**, 1315 (1999).
[25] J. Xi and C. Froese Fischer, Phys. Rev. A **59**, 307 (1999).
[26] H. L. Zhou, S. T. Manson, L. Vo Ky, A. Hibbert, and N. Feautrier, Phys. Rev. A **64**, 012714 (2001).
[27] M. Gisselbrecht *et al.*, Phys. Rev. Lett. **82**, 4607 (1999).
[28] I. Lindgren and J. Morrison, *Atomic Many-Body Theory, Series on Atoms and Plasmas*, 2nd ed.(Springer-Verlag, New York, 1986).
[29] C. deBoor, *A Practical Guide to Splines* (Springer-Verlag, New York, 1978).
[30] W. R. Johnson, S. A. Blundell, and J. Sapirstein, Phys. Rev. A **37**, 307 (1988).
[31] W. R. Johnson and J. Sapirstein, Phys. Rev. Lett. **57**, 1126 (1986).
[32] For an account of the early contributions to the complex rotation method see the complete No. 4 issue of Int. J. Quantum Chem. **14** (1978).
[33] L. B. Madsen, P. Schlagheck, and P. Lambropoulos, Phys. Rev. Lett. **85**, 42 (2000).

[34] L. B. Madsen, P. Schlagheck, and P. Lambropoulos, Phys. Rev. A **62**, 062719 (2000).
[35] Y. K. Ho, Phys. Rep. **99**, 1 (1983).
[36] G. D. Doolen, J. Phys. B **8**, 525 (1975).
[37] E. Lindroth, Phys. Rev. A **49**, 4473 (1994).
[38] D. H. Oza, Phys. Rev. A **33**, 824 (1986).
[39] A. V. Bunge and C. F. Bunge, Phys. Rev. A **30**, 2179 (1984).
[40] M. Bylicki and G. Pestka, J. Phys. B **29**, L353 (1996).
[41] E. Balslev, in *Resonances—Models and Phenomena*, edited by S. Albeverio, L. S. Ferreira, and L. Streit (Springer-Verlag, Berlin, 1984).